SARTORIUS

Application Note

Aug 3, 2020

Keywords or phrases:
Neuroscience, 3D Models, Incucyte®, Cell Analysis Systems

An Insight Into How 3D Models Can Benefit the Neuroscience Field

Introduction

Understanding the human brain and its pathological state remains one of the greatest challenges of our time. Due to the brain's great complexity and lack of suitable translational *in vitro* models, deciphering its functionality and multicellular interactions is challenging. Nevertheless, routinely used 2D cell models offer fundamental insight into the brain's biology, allowing for mechanistic behaviors and investigation of treatments. These monolayers consistently become more sophisticated by introducing further scientific advancements, both biological and technological. Recent advances in induced pluripotent stem cell (iPSC) technologies enable the humanization of neuronal models where primary cells, ahead of post-mortem tissue, are not an option. The introduction of co- and tri-cultures offer the possibility of studying cell-to-cell interactions, however, these 2D models still lack the complex organized structures taking place within a living brain. A further advancement comes from designing more sophisticated *in vitro* models that can better recapitulate the structure and pathophysiology of the brain, thus enabling deeper insight into neurological development and disease [1].

Spheroid models have the potential to derive more physiologically relevant information by exhibiting the complexity of *in vivo* tissue [2]. Due to the dynamic nature of the neuronal system and chronic nature of pathology, an enhanced translation may be obtained by coupling 3D models to long-term, time-lapse kinetic experimental data acquisition. In this Application Note we describe how 3D models can be utilized in the neuroscience area, exemplified in three areas of research: neurotoxicity [3], neuro-oncology [4], and neurodegeneration [5].

Assay Principle

In this application note we describe a simple and robust method to generate single spheroids with or without an extracellular matrix (ECM; Matrigel®). We use time-lapse imaging coupled to the automatic quantification built within the Incucyte® Live-Cell Analysis System. We combine these tools with specifically designed Incucyte® Live-Cell Reagents to obtain robust and dynamic research data to gain in-depth disease characterization and potential treatment information.

Single spheroid generation can be performed with the aid of ultra-low attachment plates (ULA). The enhanced depth of focus Brightfield (BF) image acquisition enables real-time kinetic imaging of 3D single spheroids. Characterizing spheroids and comparing phenotypes across disease lines can be performed using metrics such as speed of spheroid formation, morphology (eccentricity), or area.

Post-spheroid stabilization and following a potential drug treatment, monitoring metrics indicating cell health (with Incucyte® NucLight or CytoLight reagents), apoptotic death (with the Incucyte® Annexin V reagents) or spheroid invasiveness (by means of generating a scaffold with Matrigel®) can be performed. These data can be used to characterize diseases, gain an insight on drug mechanism of action or effect of genetic mutations, or for comparison of healthy versus disease phenotypes [6].

Materials and Methods

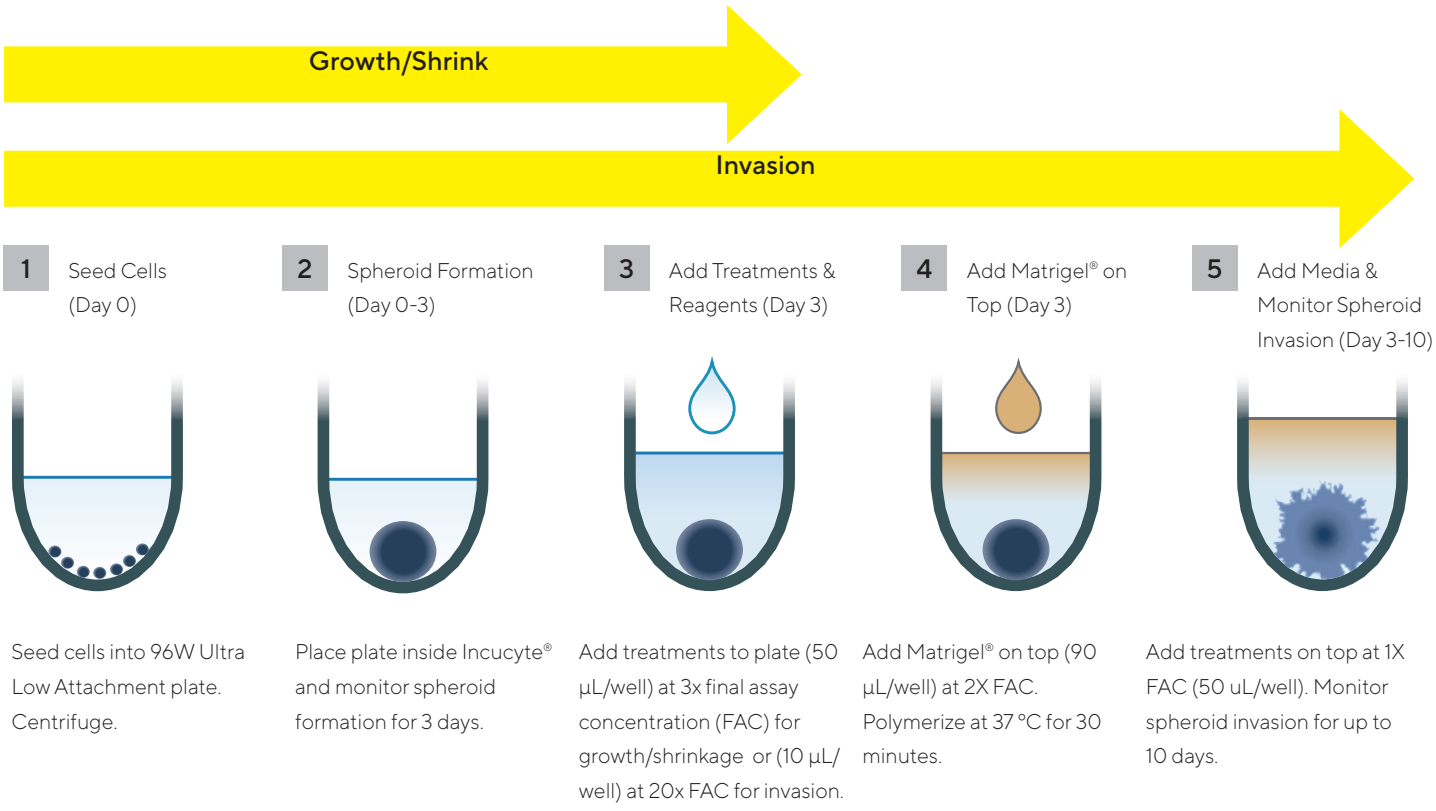

Figure 1. Assay Workflow

- Cells of interest are harvested, counted and plated into ULA round-bottom 96-well plates at desired densities (in 100 µL per well). Plates are centrifuged (125 g, 10 minutes, room temperature).
- Spheroid formation is monitored to desired size (e.g. 200-500 µm in diameter) with Brightfield and HD phase-contrast image acquisition (4x magnification) every 6 hours using the Incucyte®.
- For growth/shrink assessment, treatments and reagents can be added at this time (50 µL at 3x final assay concentration (FAC) per well).
- For invasiveness studies, treatments and reagents can be added at this time (10 µL at 20x FAC per well) followed by the addition of Matrigel® scaffold:
  - Plate is placed on a pre-chilled Coolsink 96F within a Coolbox 96F box (~ 5 minutes).
  - Matrigel® is added on top (90 µL per well at 2x FAC, e.g. 100 % for 50% FAC) and polymerized at 37°C for 30 minutes.
  - Media containing treatments at 1x FAC is added on top of the polymerized Matrigel® (50 µL per well).
- Spheroid growth/shrinkage or Invasion assays are monitored in Incucyte® (6 hour repeat scanning, for as long as your control cells remain healthy or until necessary).

All cell culture reagents were obtained from Life Technologies unless otherwise noted. U87-MG, A172, and SH-SY5Y cells (all from ATCC) were cultured in F-12K medium supplemented with 10% FBS, 1% Pen/Strep plus 1% Glutamax, with further Puromycin (0.5 µg/mL) supplementation for stably transfected nuclear labelled Incucyte® Nuclight Orange (Sartorius #4771) cell lines. Cells were grown to confluence in 75 cm^2 tissue culture treated flasks. Cells were harvested and seeded into ULA round-bottomed 96-well plates (Corning #7007) such that 3 days post cell seeding, spheroids formed with desired size. Spheroid formation was monitored in the Incucyte®, over 3 days at 6 hour intervals.

For invasion experiments, post-formation spheroids were embedded in Matrigel® (Corning #356234) at 2.25 mg/mL to induce the spheroid invasion assay. For iPSC experiments cells were obtained from Axol Bioscience (#ax0016 Healthy or #ax0112 Alzheimer's phenotypes) and differentiated according to supplier's protocol. All compounds were purchased from Tocris Bioscience and, when necessary, supplemented with the apoptotic marker Incucyte® Annexin V-NIR Dye (Sartorius #4768).

Tools to Enable Quantification of 3D Structures

To compare cell proliferation and morphology in 2D and 3D cultures, human SH-SY5Y neuroblastoma (NB) cells were seeded in 96-well flat-bottom (2D) or ULA round-bottom (3D) plates at 5,000 cells/well and centrifuged for spheroid formation. Both models were placed inside the Incucyte® Live-Cell Analysis System and phase contrast or BF images were acquired every 6 hours for 10 days at 10x or 4x magnification, respectively. Figure 2 shows representative images with associated analysis masks, demonstrating the ability to accurately segment both individual cells grown in monolayers as well as 3D spheroids. Note the linear growth characteristics in both monolayer and spheroid cultures. Near confluency is reached after 96 h in the 2D model, limiting the potential for longer term studies of modulation, whereas the 3D culture maintains linear growth even after 10 days in culture.

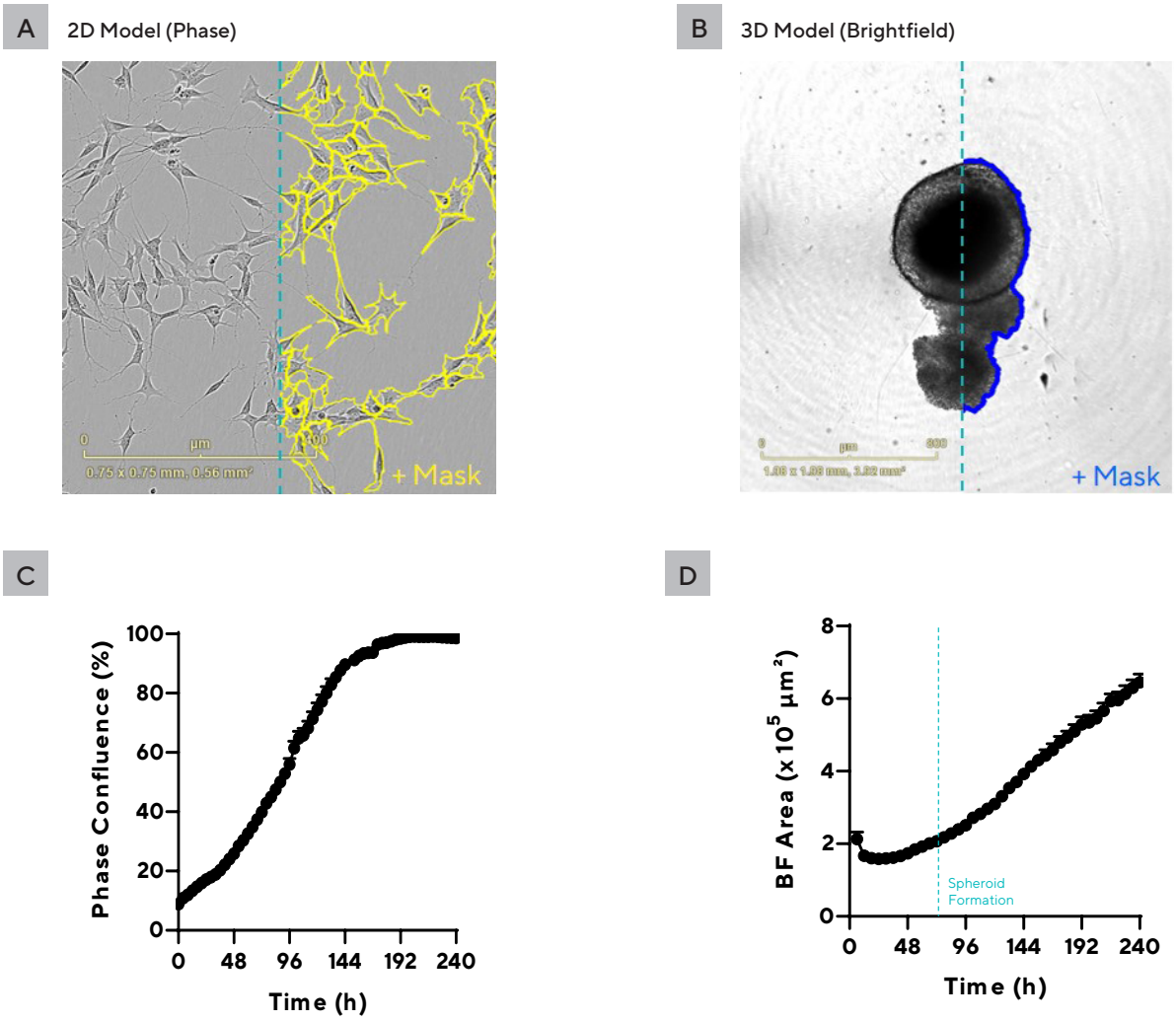

Figure 2. Monitor cell proliferation and observe morphology in 2D or 3D Cultures. Human SH-SY5Y NB cells were seeded in 96-well flat- (2D) or ULA round-bottom (3D) plates at 5,000 cells/well. Images (10x or 4x) taken every 6 h for 10 days. Representative images of cells grown as a (A) monolayer and (B) single-spheroid showing the characteristic phenotypes in both models and the segmentation masks. The time-course profiles of proliferation (C, phase confluence) or spheroid formation/growth (D, BF area). Data presented as Mean +/- SEM, 3 replicates.

In addition to BF measurements, additional properties of spheroids can also be quantified via expression of a fluorescent protein or addition of cell health reagents, such as markers of apoptosis using an Incucyte® Annexin V Dye. The human glioblastoma multiform (GBM) cell line U87-MG, stably expressing a nuclear restricted orange fluorescent protein (Incucyte® Nuclight Orange) was seeded in 96-well ULA round-bottom plates (5,000 cells/well) and centrifuged.

Images were acquired in phase, BF and orange fluorescence (FLU) every 6 hours for 10 days at 4x magnification. As expected, the BF area increased over time as the cells proliferated (Figure 3A) and importantly a similar increase in fluorescence area was attained (Figure 3B). In a separate experiment, U87-MG cells (2,500 cells/well) were seeded into 96-well ULA round-bottom plates and after 3 days of spheroid formation Matrigel® (2.25 mg/mL) was added. Invasive properties were measured using Incucyte® Single Spheroid Invasion Analysis Software, which tracks and quantifies changes in spheroid size (whole spheroid area or invading cell area) over time (Figure 3C). The time-course shows the marked increase in invading cell area, illustrating the strong metastatic potential of U87-MG cells.

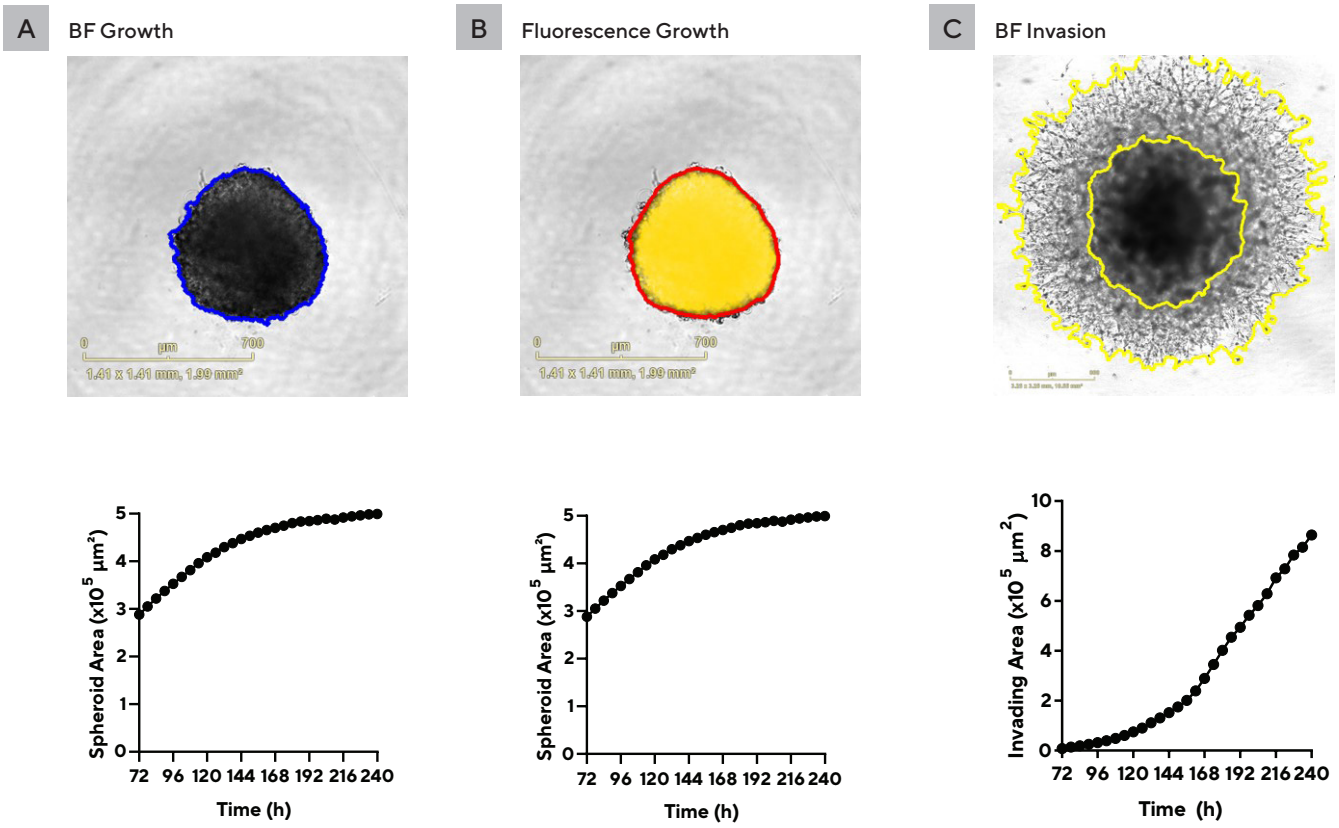

Figure 3. Quantification of spheroid growth and invasion. U87-MG cells seeded in 96-well ULA round-bottom plates (5,000 cells/well for growth and 2,500 cells/well for invasion) were allowed to form single-spheroids (3 days). Spheroid growth, monitored in the Incucyte® for 10 days, was quantified using (A) brightfield (BF) or (B) fluorescence. Spheroids embedded in Matrigel® (2.25 mg/mL) enabled the quantification of invasion (C). Data presented as Mean +/- SEM, 6-12 replicates.

Case Study 1: Neurotoxicity

A definition by the US Environmental Protection agency (EPA) of neurotoxicity is an adverse change in the structure or function of the central and/or peripheral nervous system following exposure to a chemical, physical, or biological agent [7]. Neurotoxicity is one of the main causes for withdrawal of pharmaceuticals from the market, and this field is regulated by a strict framework of guidelines [8]. In addition, the adverse effects of pharmaceuticals are poorly predicted by the current *in vitro* preclinical studies and toxicity assessment in 3D neuronal cultures may play an important role in this field [9].

Untangling the Toxic Effects of Taxol

Here we studied the effects of the chemotherapeutic compound Taxol, known to exert neuropathological outcomes in the clinic. To understand cell viability, spheroids were formed as previously described using neuronal SH-SY5Y or astrocytic U87-MG cell lines stably expressing a nuclear restricted fluorescent protein (Incucyte® Nuclight Orange). Incucyte® Annexin NIR Dye (0.5%) and treatment with Taxol were added post spheroid formation and BF and FLU images were acquired every 6 hours for 10 days.

When studying BF images, Taxol appeared to elicit differential effects on SH-SY5Y neuronal spheroids compared to U87-MG (Figure 4). The lobular appearance of vehicle treated SH-SY5Y spheroids was lost at Taxol concentrations above 0.31 µM (Figure 4A). Analysis revealed that Taxol did not yield the expected concentration-dependence, appearing to elicit less effect at higher concentrations. This observation may be related to the changes in spheroid morphology. When studying U87-MG spheroids, Taxol exerted a marked inhibition of BF area, however failed to yield a reduction comparable to the positive control camptothecin (1 µM) even at maximal concentrations (Figure 4B).

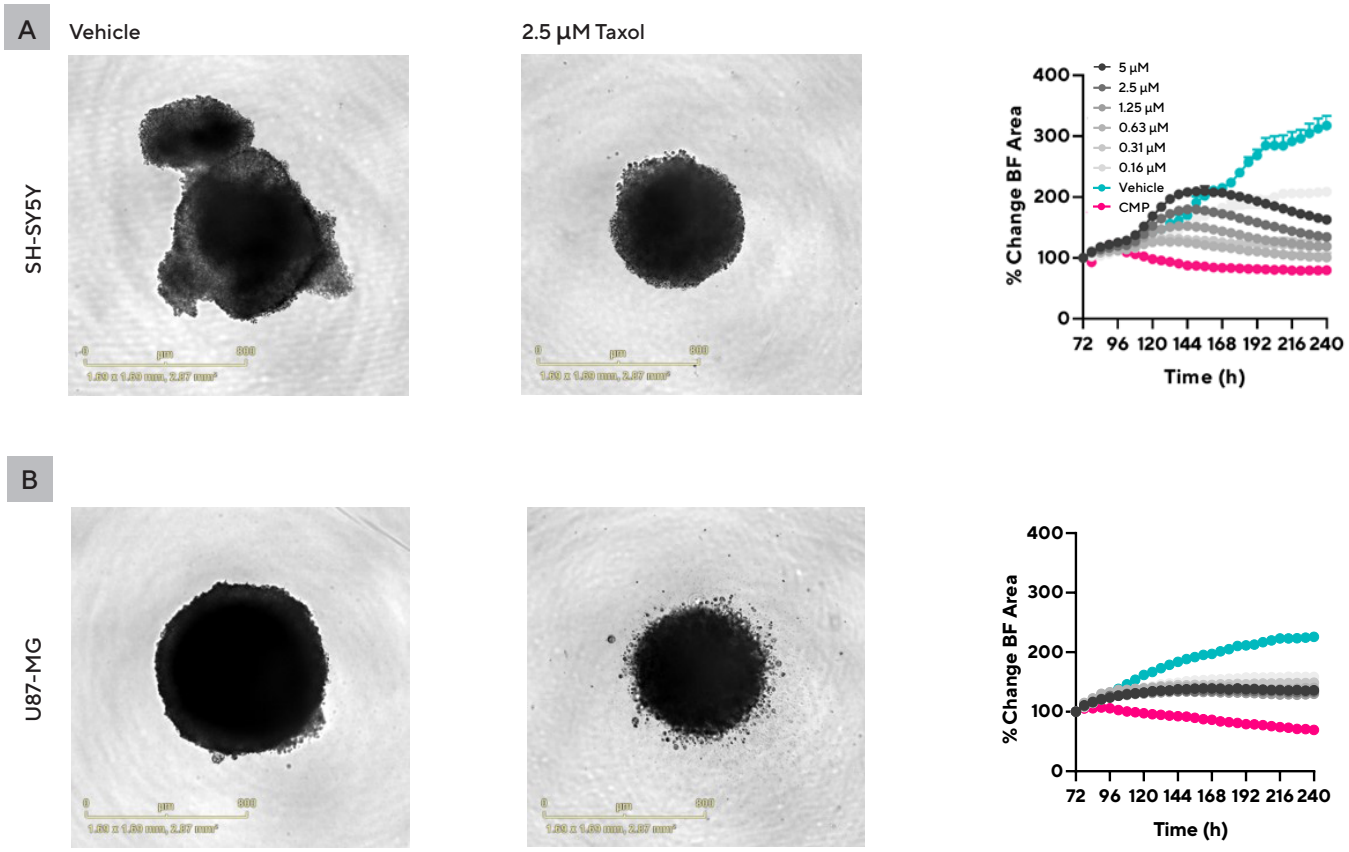

Figure 4. Effects of Taxol on brain cell types. SH-SY5Y or U87-MG cells were used to form spheroids in 96-well ULA round-bottom plates at 5,000 cells/well. Upon formation (3 days), spheroids were treated with Taxol (0.16 – 5 µM). BF images were taken every 6 h for 10 days and automatically segmented. Representative images show the BF images either treated with vehicle or Taxol (2.5 µM) after 168h. The time courses show BF area expressed as a percentage of the first time point. Data presented as Mean ± SEM, 6-16 replicates.

To address the effects of Taxol on the viability of the SH-SY5Y cells within the spheroids further analyses were performed to study fluorescent properties within the BF boundary. Taxol induced a concentration-dependent reduction in the orange fluorescent intensity and concomitant increase in NIR fluorescent intensity, consistent with a loss in viability and increase apoptosis (Figure 5B). Analysis yielded identical IC_{50} values of 0.3 µM for the loss of orange or gain in NIR intensity (Figure 5C). The use of BF combined with the cell health and viability fluorescent reagents provide a deeper insight into the specificity and neurotoxic effects of Taxol at a throughput commensurate to compound profiling.

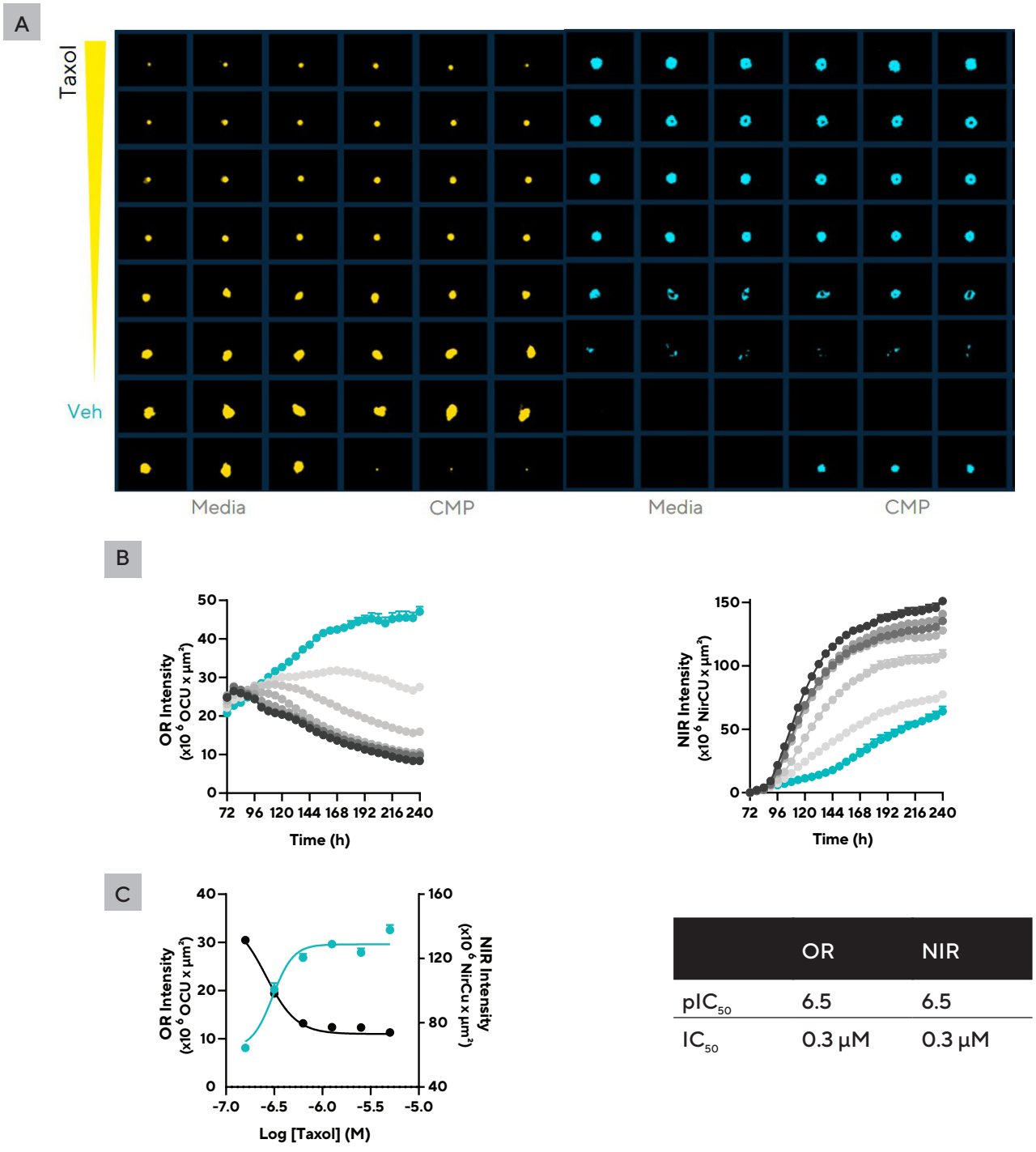

	OR	NIR
pIC_{50}	6.5	6.5
IC_{50}	0.3 µM	0.3 µM

Figure 5. Fluorescent analysis of SH-SY5Y spheroids. SH-SY5Y cells stably expressing an orange nuclear restricted protein (Incucyte® Nuclight) were used to form spheroids in 96-well ULA round-bottom plates at 5,000 cells/well. Upon formation (3 days), spheroids were treated with Taxol (0.16 – 5 µM) and Incucyte® Annexin V NIR (0.5%) Dye was added. BF and FLU images were taken every 6 h for 10 days and automatically segmented. The 96-well plate view (DeepView) shows the orange (left side) or NIR (right side) images (A). Time course profiles of the integrated orange or NIR intensity (B) and the corresponding concentration response curves (at 120 h, C). Concentration-dependent effects of Taxol was observed and the pIC_{50} and IC_{50} values are given in the table. Data presented as Mean ± SEM, 6 replicates.

Case Study 2: Neuro-Oncology

Brain cancer is one of the most aggressive and difficult-to-treat malignancies [10]. Brain tumors are a heterogeneous mass of abnormal cells growing within the rigid skull, resulting in great competition for space with healthy tissue. As with other types of solid cancers, they are complex structures in a dynamic interplay with their host and 3D models may offer improved capture of tumor biology and the chemo-resistant microenvironment of GBMs, thus improving translational value [11], [12]. Cell invasion is a hallmark of malignant cancers, clinically inhibiting this process to decrease tumorigenesis will lead to a better prognosis [13].

Characterizing Chemotherapeutic Effects on GBMs

3D growth/shrinkage models [14] were generated to characterize brain tumors. To gain insight into the mechanism of action (MoA) of two commonly used chemotherapeutic drugs, the DNA inhibitor Cisplatin and the dual mTOR inhibitor PP242, pharmacological tests combining spheroid growth/shrinkage assays with apoptotic readouts were performed in U87-MG GBMs (Figure 6). Cells were seeded (5,000 cells/well) as previously described and then treated with the drugs in media supplemented with Incucyte® Annexin VNIR Dye (0.5%) and BF and FLU images were acquired for 10 days. PP242 (5.6 µM) abolished spheroid growth (change in BF area -15% compared to pre-treatment), however, this concentration induced only moderate apoptosis (fluorescent area of ~35%). Conversely, Cisplatin (66.6 µM) induced a marked apoptotic signal (fluorescent area of 99%) while inducing a sub-maximal reduction in spheroid size (BF area of +25% compared to vehicle). Construction of concentration response curves revealed Cisplatin exhibited similar potencies on spheroid area and apoptotic signal (IC_{50} values of 4.6 and 4.4 µM, respectively), consistent with a cytotoxic mechanism of action. In contrast, PP242 appeared cytostatic, yielding 10-fold higher potency for spheroid area inhibition than apoptotic signal (IC_{50} values of < 5.9 and 4.8 µM, respectively).

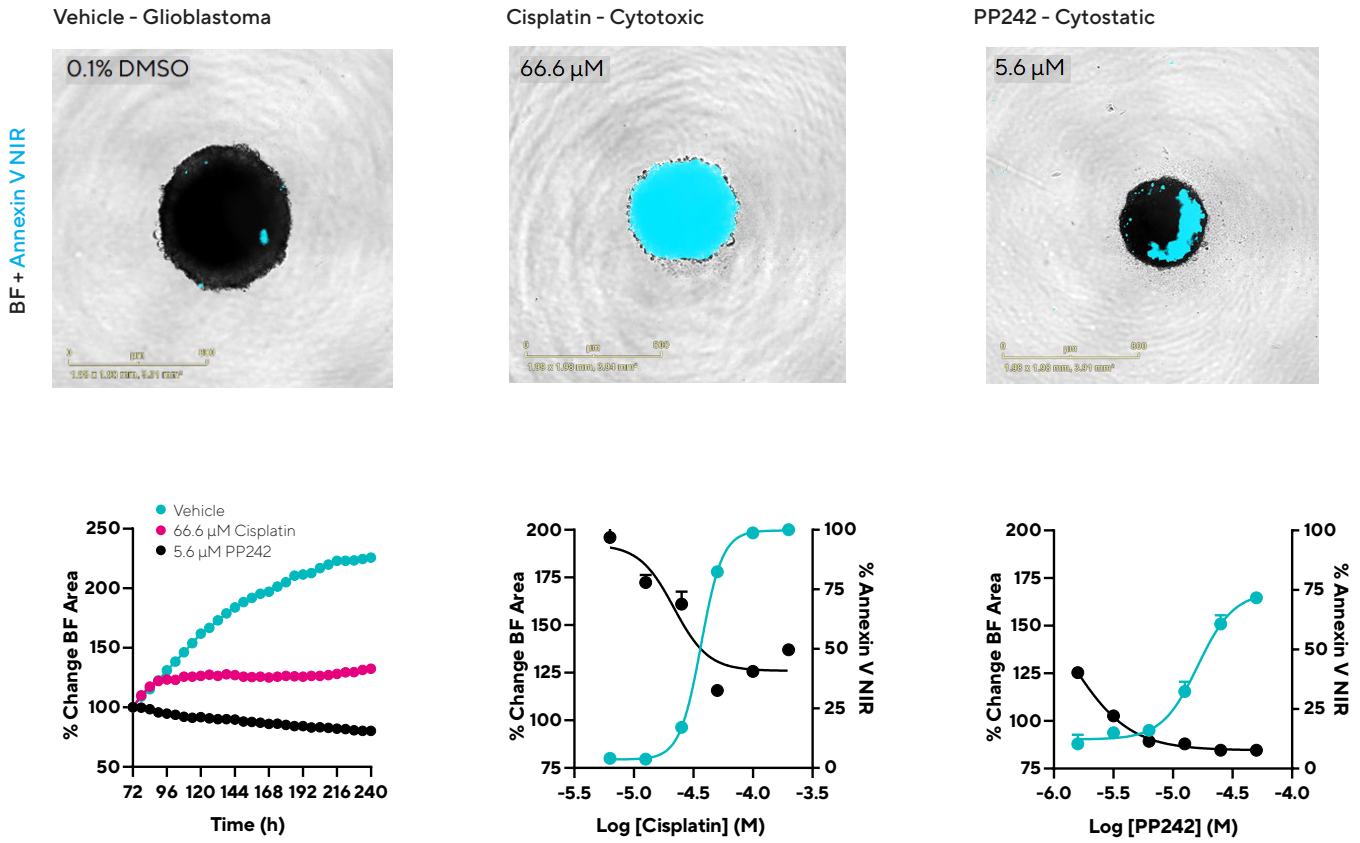

Figure 6. Differential cytostatic and cytotoxic effects of chemotherapeutic compounds. U87-MG spheroids were formed in 96-well ULA round-bottom plates at 5,000 cells/well. Upon formation (3 days), spheroids were treated with Cisplatin (0.82 – 200 µM) or PP242 (0.21 - 50 µM) in media supplemented with Annexin VNIR Dye (0.5%). 4x BF and FLU images were taken every 6 h for 10 days and automatically segmented. Metrics for % change of spheroid area from pre-treatment, or % spheroid displaying apoptosis were used to generate time-courses and concentration-response curves (3 days post-treatment). The time-course displays the % change in BF area for concentrations of Cisplatin (Pink; 66.6µM) and PP242 (Black; 5.6 µM) compared to vehicle (Teal), where data is normalized to pre-treatment to account for variation in spheroid size. Derived pIC_{50} values were consistent with a cytotoxic (drug affected spheroid size and % apoptosis similarly) or a cytostatic (greater sensitivity to drug observed in spheroid size than in % apoptosis) MoA. Data presented as Mean +/- SEM, 12 replicates.

Impact of mTOR Inhibition on Invasive Potential

Gliomas are the most common intracranial tumors in humans. From those, GBMs are the most malignant due to their high infiltrative growth into the healthy brain [15]. Invasion models [16] were generated to characterize brain tumors. The capability of invasion of U87-MG or A172 GMBs were studied by seeding 2,500 cells/well and generating spheroids for 3 days. Once formed, Matrigel® ECM was added to embed the spheroid, in addition to compound treatment. Segmentation revealed U87-MG cells readily invaded the ECM (Figure 7A+B), with an invading area of 8.6 x10^5 µm^2, whereas A172 cells showed a lower invasive capacity, yielding an invading area of 2.1 x10^5 µm^2 after 168 h (Figure 7C). Treatment with the mTOR inhibitor PP242 yielded concentration-dependent inhibition of invasion in both cell types (Figure 7D). Notably the inhibitory potency of invasion was considerably higher in A172 than U87-MG cells, yielding IC_{50} values of 0.9 µM and 6.4 µM, respectively. Despite the promising effects of PP242 to potently inhibit U87-MG spheroid growth, the data suggest only limited effects on invasion of this highly metastatic cell type.

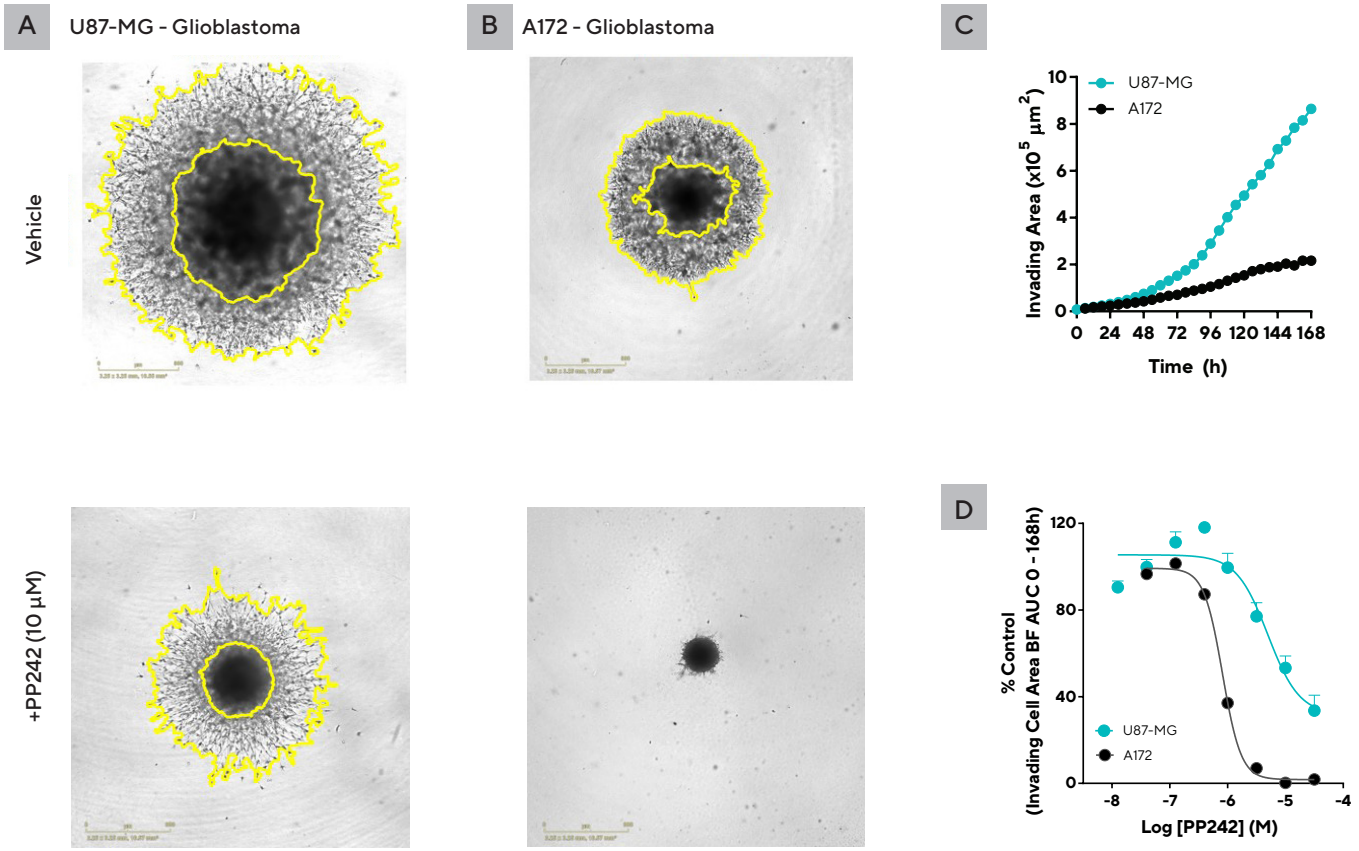

Figure 7. Differential invasive potential and impact of mTOR inhibition of GBM cell lines. U87-MG and A172 spheroids were formed in 96-well ULA round-bottom plates at 2,500 cells/well. Upon formation (3 days), Matrigel® was added and spheroids were treated with PP242 (0.01 – 30 µM). Representative images of U87-MG and A172 cells either following vehicle or PP242 (10 µM) treatment. Note the moderate impact of PP242 on U87-MG spheroids (A) and near complete abolition of invasion in A172 spheroids (B). (C) Time-course of invading area, highlighting the greater invasive capacity of U87-MG cells. (D) Concentration response analysis reveals a lower inhibitory potency of invasion in U87-MG spheroids compared to A172 spheroids (IC_{50} values of 6.4 and 0.9 µM, respectively).

Case Study 3: Neurodegeneration

Treatment of neurodegenerative disease remains an unmet clinical need, with patient numbers steadily increasing, and a global healthcare budget becoming unsustainable. Thus, there is pressure to develop more translational models. Improved disease modelling may be achieved, at least in part, by the introduction of human iPSC-derived cell types [17] in conjunction with 3D cultures [18].

Phenotypical Characterization of Health and Disease

Here we developed a 3D iPSC model of Alzheimer's disease (AD) and compared the phenotypic characteristics of a patient-derived (PSEN1 mutation) line with a healthy individual. Different size spheroids of healthy and AD iPSC cell lines (Axol Bioscience) were formed as described previously (390 - 50,000 cell/well). Spheroids were allowed to form for 3 days, when neuronal differentiation was induced as per supplier's kit protocol. BF images were taken using the Incucyte® Live-Cell Analysis System every 6 hours for up to 15 days. Time courses show the proportional increase in spheroid size with seeding density and the inverse relationship of growth potential for the AD line (Figure 8A). When the spheroid area of both the healthy and AD line were compared, the latter consistently presented an increased size for the same cell seeding density (Figure 8B). Capability of invasion and neurite development was compared for both cell types by addition of Matrigel® (2.25 mg/mL) at 6 days post spheroid formation. Neurite development was continually monitored for a further 9 days. The images show the characteristic phenotype in which AD neurons presented higher core size and lower neurite development when compared to the healthy neurons (Figure 8C).

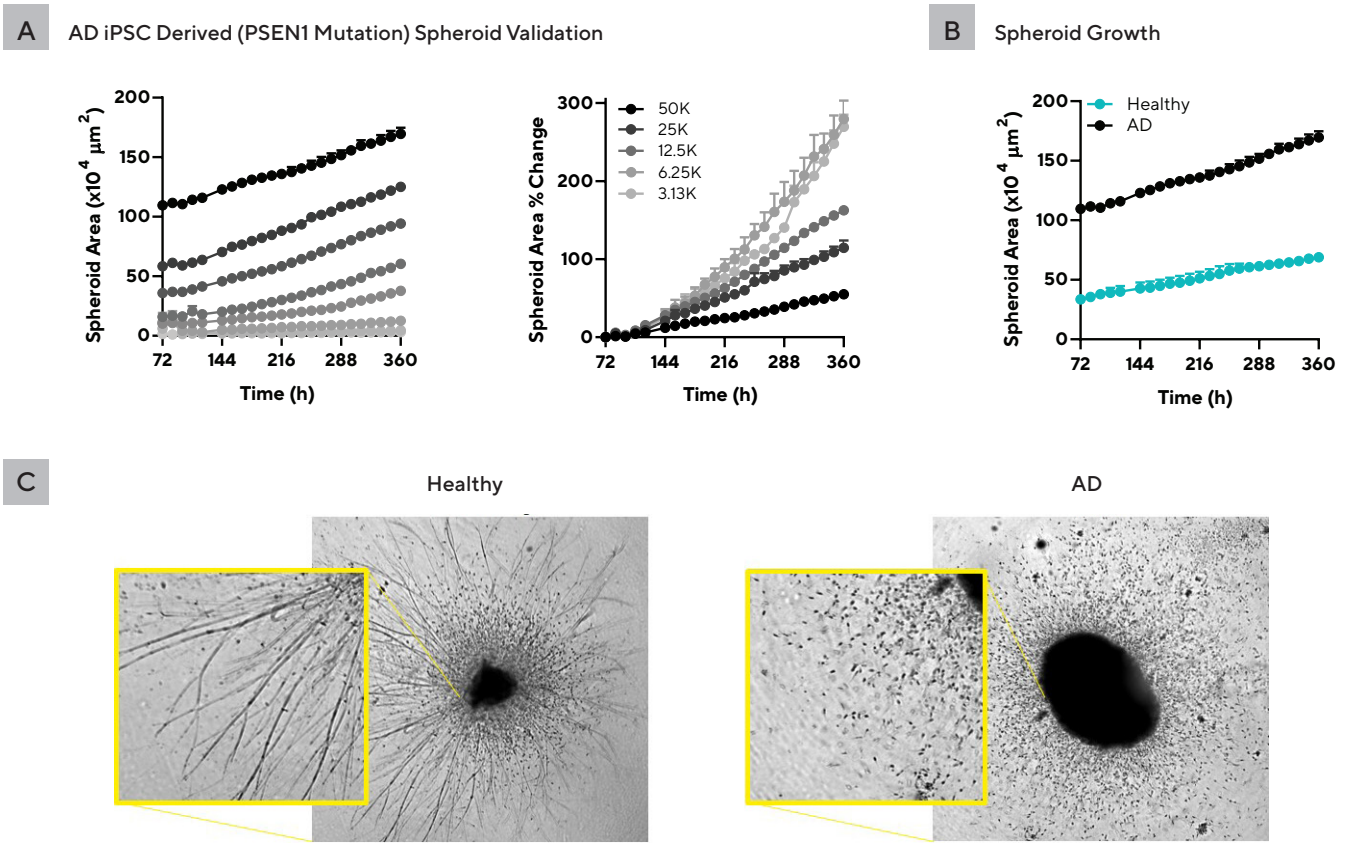

Figure 8. 3D characterization of patient-derived Alzheimer's iPSC cell line. Healthy and AD cells (Axol Bioscience) spheroids were formed in 96-well ULA round-bottom plates at a density range (390 - 50,000 cell/well). Upon formation (3 days), spheroids were differentiated as per supplier's protocol kit. 4x BF images were taken every 6 hours for 15 days and automatically segmented. Time courses show the proportional increase in spheroid size with seeding density and the inversed relation of growth potential for the AD line (A). For a similar cell density, the AD line consistently presented an increased in size (B). Capability of invasion and neurite development was compared by addition of Matrigel® (2.25 mg/mL) 6 days post-spheroid formation, and monitored for a further 9 days. The images show a larger core and a lower neurite development for AD when compared to healthy line (C). Data presented as Mean +/- SEM, 3 replicates.

Conclusion

In this application note we described the importance of developing physiologically relevant cellular tools for an improved modelling of neuronal-related disorders, which in turn may result in the advancement of drug discovery. We described:

- Live-cell analysis revealed differential modulation by a chemotherapeutic agent on spheroid growth and invasive potential.
- Live-cell analysis of spheroids highlighted cell type-specific neurotoxicity.
- Incorporation of patient-derived iPSCs with 3D organization may enable novel models of Alzheimer's Disease.

What the future brings in the field of 3D research (spheroids, neurospheres, and organoids) is only now starting to be understood. Organoids comprise an improved self-organisation that may better describe the complex structure as a miniature brain and developing more basic 3D models will provide stepping stones, both biologically and technologically. There is, however, a long way yet to go, with reproducibility of brain organoid generation [19] and characterization of these structures to elucidate disease mechanism and profile compounds. Finally, to bring bio-printing to the forefront may offer mini brains and is a new and very exciting technology currently in development [20], which may revolutionize the area of personalized medicine.

References

1. D. C. D. P. D. Y. K. D. I. Dr. Mehdi Jorfi, **Three-Dimensional Models of the Human Brain Development and Diseases**. *Advanced Healthcare Materials*, vol. 7, no. 1, 10 Jan 2018.
2. S. A. Langhans, **Three-Dimensional in Vitro Cell Culture Models in Drug Discovery and Drug Repositioning.** *Frontiers in Pharmacology*, vol. 9, p. Article 6, 23 January 2018.
3. F. P. D. N. S. S. B. S. M.-C. K. R. M. B. G. C. C. C. S. V.-H. O. G. R. G. F. Z. a. C. C. Oksana Sirenko, **Functional and Mechanistic Neurotoxicity Profiling Using Human iPSC-Derived Neural 3D Cultures**. *Toxicological Sciences*, vol. 167, no. 1, pp. 58-76, 2019.
4. K. S. L. G. G. H. a. A. J. C. Natividad Gomez-Roman, "**A novel 3D human glioblastoma cell culture system for modeling drug and radiation responses.** *Neuro-Oncology*, vol. 19, no. 2, 2017.
5. I. W. I. M. D. D. C. D. D. Y. K. Joseph Park, **A 3D human triculture system modeling neurodegenation and neuroinflammation in Alzheimer's disease**. *Nature Neuroscience*, vol. 21, pp. 941-951, 27 June 2018.
6. E. B. Sartorius, **Incucyte® 3D Tumor Spheroid Assays.** [Online]. Available: https://www.essenbioscience.com/en/applications/cell-health-viability/3d-tumor-spheroid-assays/
7. EPA/630/R-95/001F, **Guidelines for Neurotoxicity Risk Assessment**. 1998.
8. S. Z. I. R. A. R. Abigail L Walker, **Drug discovery and development: Biomarkers of neurotoxicity and neurodegeneration.** *Experimental Biology and Medicine*, vol. 243, pp. 1037-1045, 2018.
9. F. P. S. D. N. S. S. B. S. M.-C. K. R. M. B. G. C. C. C. S. V.-H. O. G. R. G. F. Z. a. C. C. Oksana Sirenko, **Functional and Mechanistic Neurotoxicity Profiling Using Human iPSC-Derived Neural 3D Cultures**. *Toxicological Sciences*, vol. 167, no. 1, pp. 58-76, 2019.
10. R. H. E. B. L. P. Herb Brody, **Brain Cancer.** *Nature Outlook*, no. 7724, 2018.
11. R. G. R. d. H. S. V. C. B. M. G. a. H. v. d. K. John A. Hickman, **Three-dimensional models of cancer for pharmacology and cancer cell biology: Capturing tumor complexity *in vitro/ex vivo*.** *Biotechnology Journal*, vol. 9, pp. 1115-1128, 2014.
12. S. W. Ahmed Musah Eroje, **A novel 3D *in vitro* model of glioblastoma reveals resistance to temozolomide which was potentiated by hypoxia**. *Journal of Neuro-oncology*, vol. 142, pp. 231-240, 2019.
13. S. L. J. S. R. K. N. C. S. S. L. Y. K. G. N. F. A. W. Y. A. P. K. D. H. D. W. C. O. M. G. F. A.-O. &. J. S. R. Sanjeeva Mohanam, **Down-regulation of cathepsin B expression impairs the invasive and tumorigenic potential of human glioblastoma cells**. *Oncogene*, vol. 20, pp. 3665-3673, 2001.
14. M. O. K. P. T. D. D. T. N. H. E. E. Susana L. Alcantara, **Label-free, real-time live-cell assays for spheroids: Incucyte bright-field analysis**. 2017. [Online]. Available: https://www.essenbioscience.com/en/applications/cell-health-viability/spheroids/
15. J. E. S. S. a. U. N. Angela Armento, Glioblastoma **(Chapter 5: Molecular Mechanisms of Glioma Cell Motility)**, vol. Chapter 5, Codon Publications, 2017.
16. K. P. S. P. N. H. S. U. T. D. Miniver Oliver, **Real-Time Live-Cell Analysis of 3D Tumor Spheroid Invasion**. 2019. [Online]. Available: https://www.essenbioscience.com/en/communications/oncology/
17. J. L. T. R. J. K. a. B. W. Katrin Simmnacher, **Modeling Cell-Cell Interactions in Parkinson's Disease Using Human Stem Cell-Based Models.** *Frontiers in Cellular Neuroscience*, vol. 13, p. 571, 2020.
18. [18] H. C. a. A. B. Eduarda G Z Centeno, **2D versus 3D human induced pluripotent stem cell-derived cultures for neurodegenerative disease modelling.** *Molecular Neurodegeneration*, vol. 13, no. 27, 2018.

19. A. J. K. S. K. S. A. N. M. R. G. Q. B. P. L. N. X. A. A. R. J. Z. L. &. P. A. Silvia Velasco, "Individual brain organoids reproducibly form cell diversity of the human cerebral cortex," *Nature Letters,* vol. 570, pp. 523-527, 03 June 2019.
20. P. Hao-Wei Han and Shan-hui Hsu, "Using 3D bioprinting to produce mini-brain," *Neural Regeneration Research,* vol. 10, pp. 1595-1596, 2017.
21. H. Setia and A. R. Muotri, "Brain organoids as a model system for human neurodevelopment and disease.," *Seminars in cell & develomental biology*, vol. 95, no. 5, 9 March 2020.
22. A. S. A. M. V. P. L. G. A. V. G. & T. S. Maria Louca, "Ras suppressor-1 (RSU-1) promotes cell invasion in aggressive glioma cells and inhibits it in non-aggressive cells through STAT6 phospho-regulation," Nature Scientific Reports, vol. 9, p. 7782, 2019.
23. C. -. E. r. results, "NeuroDeRisk - Grant ID: 821528," Horizon 2020, https://neuroderisk.eu/.

Sales and Service Contacts

For further contacts, visit www.sartorius.com

Germany
Sartorius Lab Instruments GmbH & Co. KG
Otto-Brenner-Strasse 20
37079 Goettingen
Phone +49 551 308 0

USA
Sartorius Corporation
565 Johnson Avenue
Bohemia, NY 11716
Phone 1.631.254.4249

Status: 08 | 2020